

# Anillin and the Septins Promote Asymmetric Ingression of the Cytokinetic Furrow

Amy Shaub Maddox,<sup>1,\*</sup> Lindsay Lewellyn,<sup>1,2</sup> Arshad Desai,<sup>1</sup> and Karen Oegema<sup>1,\*</sup>

<sup>1</sup>Ludwig Institute for Cancer Research, Department of Cellular and Molecular Medicine (UCSD), CMM-East Rm. 3053, 9500 Gilman Drive, La Jolla, CA 92093, USA

<sup>2</sup>Affiliated with the UCSD Biomedical Sciences Graduate Program

\*Correspondence: amaddox@ucsd.edu (A.S.M.), koegema@ucsd.edu (K.O.)

DOI 10.1016/j.devcel.2007.02.018

## SUMMARY

During cytokinesis, constriction of a cortical contractile ring generates a furrow that partitions one cell into two. The contractile ring contains three filament systems: actin, bipolar myosin II filaments, and septins, GTP-binding hetero-oligomers that polymerize to form a membrane-associated lattice. The contractile ring also contains a potential filament crosslinker, Anillin, that binds all three filament types. Here, we show that the contractile ring possesses an intrinsic symmetry-breaking mechanism that promotes asymmetric furrowing. Asymmetric ingression requires Anillin and the septins, which promote the coalescence of components on one side of the contractile ring, but is insensitive to a 10-fold reduction in myosin II levels. When asymmetry is disrupted, cytokinesis becomes sensitive to partial inhibition of contractility. Thus, asymmetric furrow ingression, a prevalent but previously unexplored feature of cell division in metazoans, is generated by the action of two conserved furrow components and serves a mechanical function that makes cytokinesis robust.

## INTRODUCTION

Cytokinesis completes cell division by physically remodeling the mother cell to partition an equal complement of the replicated genome into each daughter cell (reviewed in Glotzer, 2005; Robinson and Spudich, 2004). Following chromosome segregation, the anaphase spindle signals to the cortex to elicit the assembly of an actomyosin-based contractile ring around the cell equator between the segregated chromosomes. Constriction of the contractile ring deforms the equatorial cortex to generate a furrow consisting of back-to-back plasma membranes. Furrow ingression gradually closes the cytoplasmic connection between the daughter cells until only a narrow bridge connects the two. Abscission is accomplished by membrane fusion at the cell-cell bridge, generating two topologically distinct cells.

The contractile ring contains three polymeric structural components: actin, myosin II, and the septins. Bipolar filaments assembled from the motor protein myosin II use the energy of ATP hydrolysis to bind and exert force on actin filaments, powering ring constriction (Glotzer, 2005; Robinson and Spudich, 2004; Satterwhite and Pollard, 1992). The septins are conserved GTP-binding proteins that form hetero-oligomers containing multiple septin polypeptides. In vitro, septin hetero-oligomers polymerize to form 10 nm filaments that can associate laterally to form higher-order assemblies (Field et al., 1996; Frazier et al., 1998; Kinoshita et al., 2002). In budding yeast, the septins form a membrane-associated filament lattice (Rodal et al., 2005; Vrabioiu and Mitchison, 2006) that directs the recruitment of other contractile ring components and is essential for cell cycle regulation, cell shape, and cytokinesis (Gladfelter et al., 2001; Hartwell, 1971). The septins also concentrate in the contractile ring in fission yeast and in animal cells (Kinoshita, 2006; Versele and Thorner, 2005); however, their function in these systems is much less clear. In *S. pombe*, septin null mutants are viable; in cells lacking septin function, the contractile ring assembles and closes normally, but cell-cell separation is delayed, suggesting a role in degradation of the primary septum (Berlin et al., 2003; Longtine et al., 1996; Tasto et al., 2003). Cytokinesis failures have been observed in some *Drosophila* tissues homozygous for a mutation in the septin gene *Peanut*, but cell divisions in other tissues were not affected (Adam et al., 2000; Neufeld and Rubin, 1994). In *C. elegans*, embryonic cytokineses are successful following inhibition of either or both of the *C. elegans* septins by RNAi or mutation (Maddox et al., 2005; Nguyen et al., 2000).

A conserved potential filament crosslinker, Anillin, also concentrates in the contractile ring. Mutations in *Anillin* result in failure of cytokinesis in *Drosophila* tissues (Field et al., 2005), and analysis of cytokinesis after depletion of Anillin by RNAi in cultured *Drosophila* (Echard et al., 2004; Somma et al., 2002) and human cells (Straight et al., 2005; Zhao and Fang, 2005) has suggested a role in stabilizing the contractile ring late in cytokinesis. Metazoan anillins bind directly to actin, myosin II, and septin filaments in vitro via distinct domains (Field and Alberts, 1995; Kinoshita et al., 2002; Straight et al., 2005). The interaction of Anillin with the septins is mediated by an extended C-terminal PH domain (Field and Alberts, 1995; Kinoshita et al., 2002; Oegema et al., 2000), and

the N terminus contains regions that can bind activated myosin II and bind and bundle actin filaments. These features make Anillin ideally suited to crosslink the actomyosin and septin cytoskeletons within the contractile ring, although functional evidence for this role is still lacking. In *S. pombe*, the ability to interact with actomyosin and the septins appears to be split between two proteins with homology to Anillin, Mid1p (Motegi et al., 2004; Sohrmann et al., 1996) and Mid2p (Berlin et al., 2003; Tasto et al., 2003), which contribute to different aspects of cytokinesis.

Asymmetric furrowing is a prevalent but mechanistically unexplored phenomenon in which the contractile ring cuts across the division plane unilaterally, rather than with circumferential symmetry. Asymmetric furrowing has been documented in polarized cultured mammalian epithelia (Reinsch and Karsenti, 1994) and in embryonic cell divisions in a variety of species (Rappaport, 1996). During epithelial cell divisions, asymmetric furrow ingression is proposed to allow maintenance of cell-cell contacts and the integrity of the epithelial barrier during the division of its constituent cells. During rapid embryonic cell divisions, asymmetric furrowing could also confer an advantage by quickly placing a barrier between the segregated masses of chromatin. Here, using the *C. elegans* early embryo to explore the mechanism of asymmetric furrowing, we show that Anillin and the septins break the symmetry of the actomyosin cytoskeleton within the contractile ring. Structural asymmetry leads to the unilateral ingression of an asymmetric furrow that is resistant to mechanical challenges.

## RESULTS AND DISCUSSION

### Anillin and the Septins Are Required for the Geometry of Furrow Ingression but Not Its Rate

To explore the interplay among actomyosin, Anillin, and the septins during cytokinesis, we compared furrow closure in control embryos to that in embryos depleted of Anillin or the septins by RNA-mediated interference (RNAi). Furrowing was monitored by imaging embryos expressing a GFP fusion with a PH domain that binds a phospholipid specifically produced on the plasma membrane (Audhya et al., 2005). The opening between the nascent daughter cells closed with similar kinetics in all cases (Figures 1A and 1B). However, there was a striking change in the geometry of furrowing in the depleted embryos. In control embryos furrow ingression was asymmetric. Initially, a shallow furrow encircled the cell equator (Figure 1A, orange arrows). Subsequently, the surface on one side of the embryo buckled inward, generating a furrow composed of two back-to-back membranes (a “doubled-membrane” furrow) that ingressed unilaterally (Figure 1A, pink arrow). Only after the halfway point of closure did a doubled-membrane furrow form and begin to ingress from the opposite side of the cell (Figure 1A, cyan arrow). In contrast to the pronounced asymmetry in control cells, a doubled-membrane furrow formed simultaneously around the embryo circumference in embryos

depleted of Anillin, the septins, or both, and furrow ingression was symmetric within the division plane (Figure 1A). It is important to note that the asymmetry of furrowing we describe here is distinct from “asymmetric cell division” in which the division plane is placed asymmetrically along anterior-posterior axis of the cell to generate daughter cells of differing size and/or fate (Gönczy and Rose, 2006). Consistent with this distinction, Anillin and the septins are dispensable for anterior-posterior axis determination (Maddox et al., 2005; Nguyen et al., 2000).

As in mammalian epithelial cells (Reinsch and Karsenti, 1994) (Figure 1C), furrowing during the first division of the *C. elegans* embryo is asymmetric despite a centrally positioned spindle (Figure 1D), indicating that asymmetry within the division plane is not due to a biased contractile ring assembly-promoting signal. A survey of the *C. elegans* early embryo indicated that furrowing is asymmetric within the division plane during all divisions of early embryogenesis (data not shown). However, the first embryonic division is the only case in which no potentially confounding factors, such as cell-cell adhesions or spindle placement eccentrically within the division plane, exist and a mechanism intrinsic to the cortical contractile ring, involving Anillin and septins, can be defined.

### Asymmetric Furrowing Requires Anillin and the Septins

To quantitatively compare ingression asymmetry following different perturbations, we generated an “end-on” view of the division plane by projecting computationally rotated 4D image series (Figure 2A; Movie S1 [see the Supplemental Data available with this article online]). At the 50% closure point, we calculated an “asymmetry parameter” equal to the maximum distance between the contractile ring and the embryo surface divided by the equivalent distance on the opposite side of the ring (Figure 2B). This parameter is 1.0 for symmetric ingression and >1.0 for asymmetric ingression. In contrast to control embryos, where the average value of the asymmetry parameter was 3.9, indicating that essentially all ingression had occurred from one side, the asymmetry parameter was significantly lower in embryos depleted of Anillin, the septins, or both (averages = 1.6, 1.6, and 1.5, respectively; Figure 2B). The axis of furrowing was random with respect to the plane of the coverslip (Movie S2), and asymmetric ingression was also observed in embryos not under compression (Figure S1; Movie S3). Since the plane of furrow ingression is perpendicular to the anterior-posterior axis of the embryo, it seemed possible that furrow asymmetry is related to dorsal-ventral axis determination. However, the direction of furrowing did not correlate with the subsequent orientation of the dorsal-ventral axis (Figure S2), which can first be scored at the four-cell stage (Gönczy and Rose, 2006).

### Asymmetric Ingression Occurs over a Wide Range of Myosin II Levels

Since myosin II is required for constriction of the contractile ring, we assessed its role in furrow asymmetry by

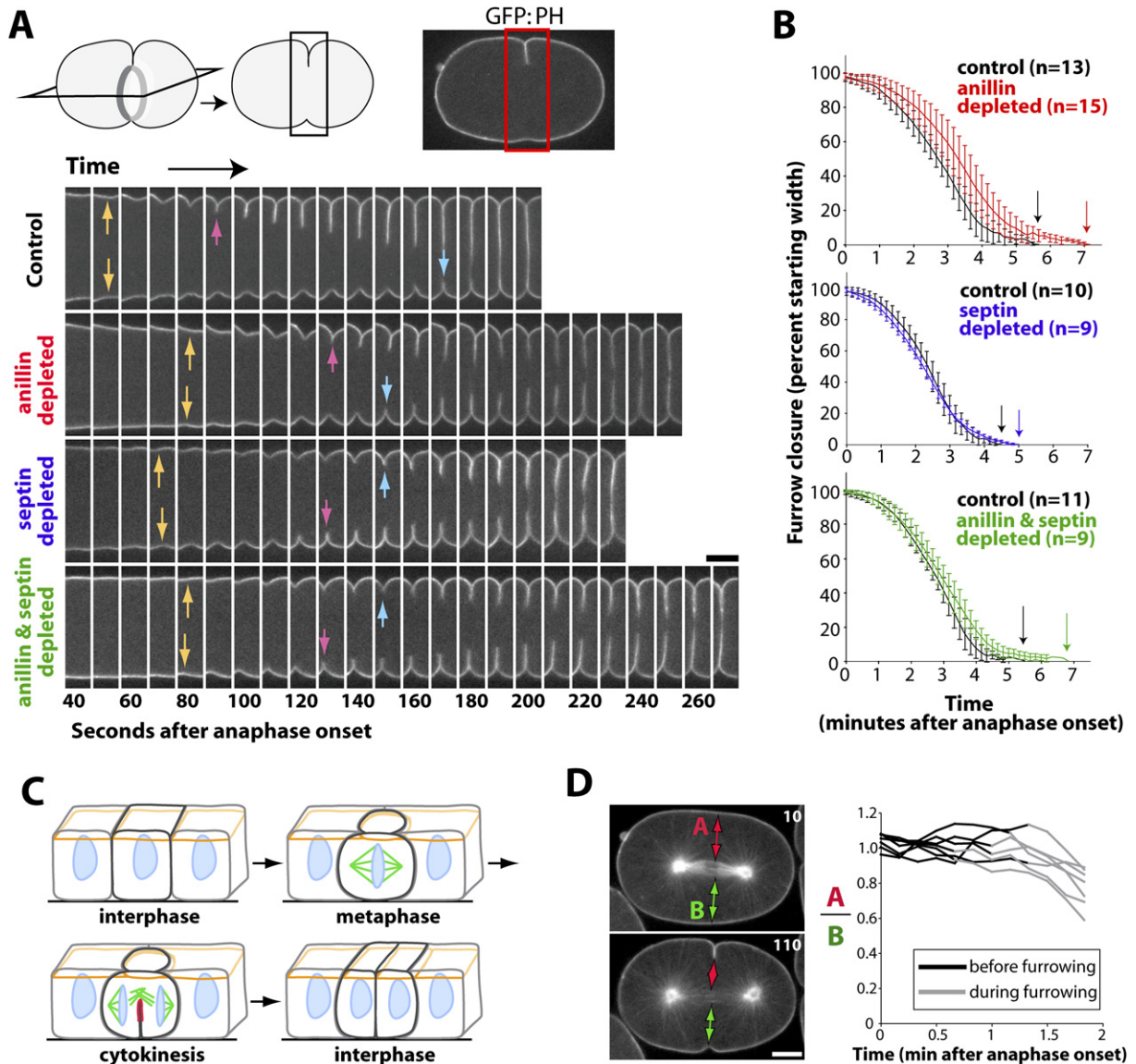


**Figure 1. Depletion of Anillin or the Septins Alters the Geometry, but Not the Rate, of Furrow Ingression**

(A) Single central plane confocal images of the cell equator from time-lapse sequences of embryos expressing a GFP-labeled plasma membrane probe. Montages show a control embryo and embryos in which Anillin (ANI-1, the *C. elegans* Anillin present in embryos [Maddox et al., 2005], referred to throughout as “Anillin”; red), the septins (UNC-59 and UNC-61; blue), or both Anillin and the septins (ANI-1 and UNC-59; green) were depleted. Scale bar = 5  $\mu$ m.

(B) Graphs showing the kinetics of contractile ring closure. The average percent starting furrow width is plotted as a function of time for each condition. Control embryos were imaged in parallel for each perturbation. Error bars = standard deviation. Cytokinesis completion (vertical arrows) was slightly delayed by the depletions.

(C) Schematic illustrating cleavage in polarized cultured MDCKII epithelial cells. The furrow (red) ingresses asymmetrically from the basal to the apical side of the cell (orange: apical junction complexes; green: spindle; blue: DNA); adapted from Reinsch and Karsenti (1994).

(D) Left: Selected images from a time-lapse sequence of an embryo coexpressing GFP: $\alpha$ -tubulin and the GFP-labeled plasma membrane probe. Times are seconds after anaphase onset. Right: The ratio of the distances A and B prior to (black) and during (gray) furrowing is plotted versus time for seven control embryos. Scale bar = 10  $\mu$ m.

analyzing embryos in which cortical myosin levels were reduced by partial depletion of its regulatory light chain, MLC-4. The amount of myosin II in the contractile ring and the asymmetry parameter were both measured in the same embryos expressing a GFP fusion with myosin

II heavy chain (NMY-2:GFP). The amount of myosin in the contractile ring was quantified from images of the cortex collected during contractile ring assembly and early constriction, and the asymmetry parameter was subsequently measured from full Z series collected during

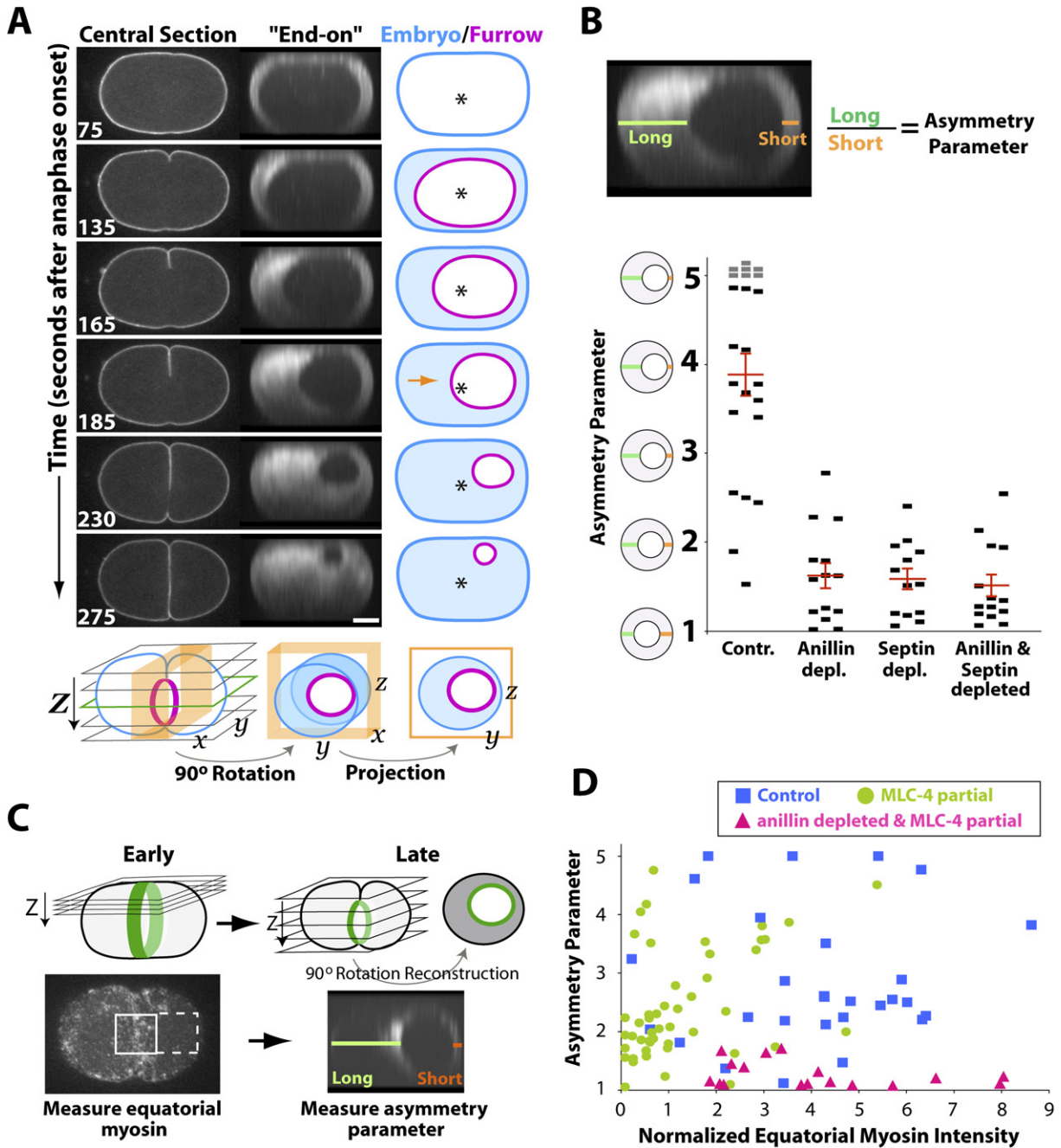


**Figure 2. Asymmetric Furrowing Requires Anillin and the Septins but Is Insensitive to Alterations in Myosin II Levels**

(A) Stills from a time-lapse sequence of a control embryo expressing a GFP-labeled plasma membrane probe. A central confocal section (left; green in schematic), projected "end-on" view of the division plane (center), and traces (right) of the embryo surface (blue) and contractile ring (pink) are shown for each time point. Asterisks mark the center of the division plane. Times = seconds after anaphase onset.

(B) The asymmetry parameter was measured as illustrated when the contractile ring was half of its initial diameter. Since small values for the length of the short axis become difficult to measure precisely, values of the asymmetry parameter greater than 5 were set to 5 (marked in gray). Red bars = average  $\pm$  SEM. Each depleted condition was significantly different from control ( $p < 10^{-7}$ ), but there was no significant difference among the depleted conditions ( $p > 0.5$ ).

(C) The amount of myosin (NMY-2:GFP) in the contractile ring was quantified in projections of four-plane Z series of the embryo cortex collected 1.5 min after anaphase onset by measuring the total GFP intensity in a box at the cell equator (solid line) after subtracting the background in a same-sized box outside the contractile ring (dotted line). The asymmetry parameter was subsequently measured from full Z series acquired during closure.

(D) The amount of myosin II in the contractile ring (arbitrary units) is plotted versus the asymmetry parameter for control embryos (blue), embryos in which myosin levels were reduced by partial depletion of its regulatory light chain, MLC-4 (green), and embryos simultaneously depleted of Anillin and partially depleted of MLC-4 (pink).

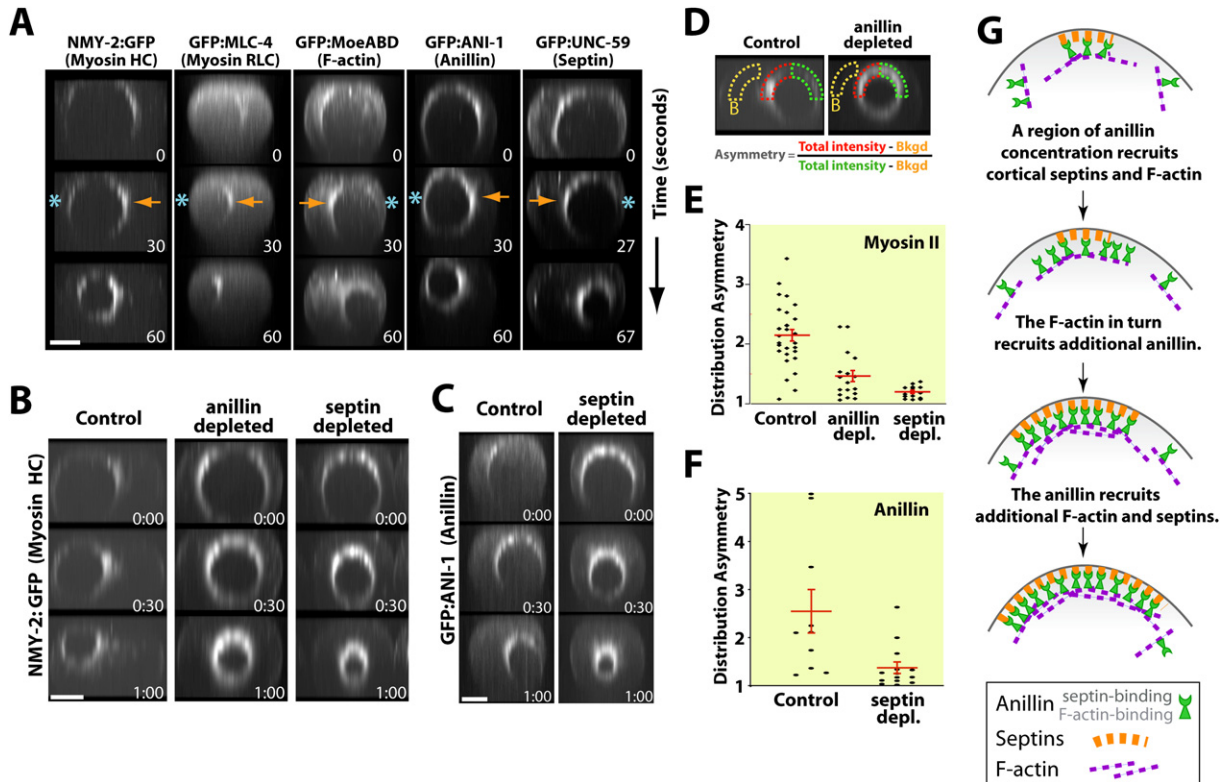


**Figure 3. Asymmetric Contractile Ring Structure Correlates with Asymmetric Furrowing**

(A) Stills from time-lapse sequences showing an end-on view of embryos expressing the indicated GFP fusions. The side of the contractile ring that has ingressed the furthest (arrows) and the opposite side of the ring (asterisks) are indicated. Times = seconds after acquisition of the first image in each sequence.

(B) End-on views of the division plane in control, Anillin-depleted, and septin-depleted embryos expressing a GFP fusion with the myosin II heavy chain (NMY-2:GFP).

(C) End-on views of control and septin-depleted embryos expressing a GFP fusion with Anillin (GFP:ANI-1).

(D) The asymmetry in the distribution of components around the contractile ring was measured by calculating the ratio between the intensities in arcs spanning the top two quadrants (red and green) of the contractile ring after subtraction of background (B; yellow).

(E and F) Measured values for the distribution asymmetry of GFP:NMY-2 (E) and GFP:ANI-1 (F) under the indicated conditions. Red bars = average  $\pm$  SEM.

(G) Model for the role of the septins and Anillin in promoting contractile ring asymmetry. See text for details. Red bars = average  $\pm$  SEM.

Scale bars = 10  $\mu$ m.

closure (Figure 2C). Myosin levels could be reduced  $\sim$ 10-fold before inhibition of furrowing precluded measurement of asymmetry. Over this wide range, there was only a small effect on the distribution of the asymmetry parameter. Statistical comparison of the asymmetry parameter distribution in control embryos with an equatorial myosin II intensity greater than 4 ( $n = 17$ ; average 2.85, range 1.5–5.0, SD = 0.96) to that in MLC-4 partially depleted embryos with measured equatorial myosin II less than 0.5 ( $n = 12$ ; average 2.1, range 1.0–4.0, SD = 0.89) revealed a wide distribution of asymmetry parameter values under both conditions and only a small shift in the parameter average (Figure 2D;  $p > 0.044$ ). We conclude that quantities of myosin II that can accomplish furrowing are also sufficient to drive asymmetric ingression. Due to its role in ingression, additional experimental approaches are needed to determine if myosin II, like Anillin and the septins, plays a role in generating asymmetry in the contractile ring. Correlation

of myosin abundance in the contractile ring and asymmetry parameter in embryos depleted of Anillin or the septins confirmed that Anillin and the septins are required for furrow asymmetry over a wide range of myosin levels (Figure 2D; Figure S3).

#### Anillin and the Septins Promote the Coalescence of Components on One Side of the Contractile Ring

To understand how Anillin and the septins promote asymmetric furrowing, we analyzed their requirement for the distribution of contractile ring components around its circumference. To generate an end-on view, time-lapse Z series of embryos expressing GFP fusions with the heavy (NMY-2:GFP) and regulatory light (GFP:MLC-4) chains of myosin II, Anillin (GFP:ANI-1), the septins (GFP:UNC-59), and the actin-binding domain of *Drosophila* moesin (GFP:MoeABD), a probe for filamentous actin (Motegi et al., 2006), were computationally rotated and projected. All of

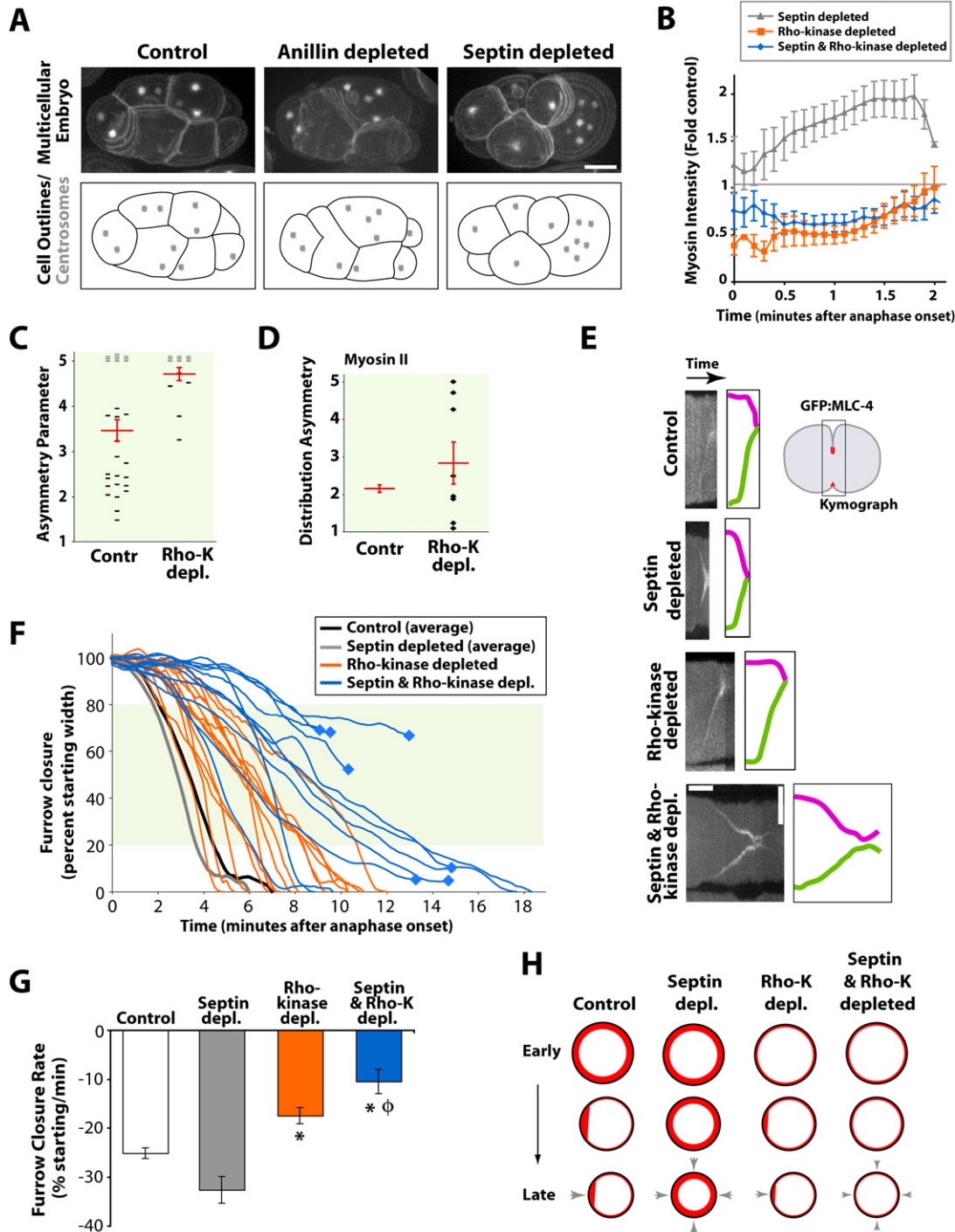


**Figure 4. Disrupting Asymmetry by Septin Depletion Renders Cytokinesis Less Robust to Inhibition of Contractility**  
 (A) Anillin- and septin-depleted embryos exhibit a low rate of stochastic cytokinesis failure (for details see text). A control embryo and embryos in which Anillin or the septins were depleted, expressing GFP fusions marking the plasma membrane (GFP:PH) and centrosomes (GFP:tubulin), are shown. Images are projections of 16-plane Z series acquired through the embryo.  
 (B) Levels of myosin (NMY-2:GFP) in the contractile ring were measured as for Figure 2C. The average myosin intensity is plotted as a function of time. Error bars = SEM.  
 (C) The asymmetry parameter was measured as for Figure 2B for control and Rho-kinase-depleted embryos expressing NMY-2:GFP. Red bars = average  $\pm$  SEM.  
 (D) The distribution asymmetry of GFP:NMY-2 in embryos depleted of Rho-kinase. The control value is from Figure 3E. Red bars = average  $\pm$  SEM.  
 (E) Kymographs of the furrow region during closure in representative embryos expressing GFP:MLC-4 for each of the indicated conditions. Horizontal bar = 5 min, vertical bar = 10  $\mu$ m.  
 (F) Furrow closure (percent starting width) vs Time (minutes after anaphase onset).  
 (G) Furrow Closure Rate (% starting/min) for Control, Septin depl., Rho-kinase depl., and Septin & Rho-K depl. conditions.  
 (H) Schematic diagrams of embryos at Early and Late stages for the four conditions.

these components were asymmetrically distributed around the contractile ring, with their highest concentration on the side of the ring that had ingressed the furthest (Figure 3A). The asymmetric distribution was apparent as soon as ingression was detectable and persisted throughout constriction. Costaining of fixed embryos confirmed the overlapping asymmetric distribution of the endogenous proteins (data not shown). Thus, the contractile ring in control embryos is structurally asymmetric, reflecting the asymmetry of furrowing. By contrast, following depletion of Anillin or the septins, myosin II was symmetrically distributed around the contractile ring (Figure 3B; Movie S4). Measurement at the half-point of closure in control cells revealed an approximately 2.0-fold higher concentration of myosin II on the side of the ring that had ingressed the furthest (Figures 3D and 3E). The asymmetry of myosin distribution was lost when either Anillin or the septins were depleted. In Anillin-depleted embryos, the septins localize to the cortex but fail to concentrate in the contractile ring (Maddox et al., 2005). In septin-depleted embryos, Anillin still concentrated in the contractile ring (Maddox et al., 2005) but was symmetrically distributed (Figures 3C and 3F).

Cumulatively, these results suggest that Anillin recruits the septins to the contractile ring where they break its symmetry and promote its asymmetric closure. We postulate that Anillin and the septins stabilize and amplify an initial stochastic asymmetry in the cortical cytoskeleton, causing it to coalesce on one side of the ring (Figure 3G). In this model, an initial asymmetry in the distribution of Anillin causes a local accumulation of actin filaments and cortical septin filament assemblies analogous to the septin “gauzes” characterized by electron microscopy in budding yeast (Rodal et al., 2005). The septin and actin polymers, in turn, recruit additional Anillin. Thus, by cross-linking the actomyosin cytoskeleton to the septins, Anillin generates a potent positive feedback loop that clusters the structural components of the contractile ring.

#### Asymmetric Furrowing Serves a Mechanical Function, Making Cytokinesis Robust to Partial Inhibition of Contractility

What is the function of furrow asymmetry? One possibility is that asymmetric furrowing confers a mechanical benefit that makes cytokinesis robust. To test this idea, we compared the rate of cytokinesis failure in control embryos to that in Anillin- or septin-depleted embryos. We examined embryos that had undergone multiple rounds of cell division (>8 cell stage) that were expressing GFP fusions to mark the plasma membrane and centrosomes. In control embryos, each cell had the proper number of centro-

somes (one or two depending on cell cycle stage,  $n > 480$  cells in 60 embryos). Among 54 Anillin-depleted multicellular embryos, 6 cells contained more than two centrosomes (Figure 4A;  $\sim 1.3\%$  failure rate;  $n > 450$  cells;  $p = 0.003$ ). Similarly, two cells that had failed cytokinesis were observed in 45 septin-depleted embryos (Figure 4C;  $\sim 0.6\%$  failure rate;  $n > 350$  cells;  $p = 0.048$ ). No pattern in the cell type among failed cells was noted. These results suggest that while Anillin or the septins are not essential for embryonic cytokinesis in *C. elegans* (Maddox et al., 2005; Nguyen et al., 2000), they make it robust to stochastic errors.

To test whether symmetrically ingressing furrows are mechanically less robust, we decreased myosin levels in the contractile ring while simultaneously inhibiting furrow asymmetry. We depleted the septins rather than Anillin for this experiment because Anillin-depleted embryos exhibit defects in addition to failure of furrow asymmetry (such as reduced cortical ruffling during pronuclear migration [Maddox et al., 2005]), whereas septin null embryos do not exhibit other detectable embryonic phenotypes (Nguyen et al., 2000). Myosin recruitment to the contractile ring was decreased by depletion of Rho-kinase (Figure 4B), a Rho effector that activates myosin by promoting the phosphorylation of its regulatory light chain (Matsumura, 2005; Piekny and Mains, 2002). As expected (Matsumura, 2005; Piekny and Mains, 2002), depletion of Rho-kinase slowed the rate of furrow ingression (Figure 4G), but cytokinesis was always successful (Figure 4F;  $n = 16$ ; identical results for embryos from two other strains; data not shown). In Rho-kinase-depleted embryos, both furrow ingression and the distribution of myosin within the contractile ring were asymmetric, to an even greater degree than in controls (Figures 4C and 4D). When the septins and Rho-kinase were simultaneously depleted, furrowing was symmetric (Figure 4E), and myosin levels were similar to those in embryos depleted of Rho-kinase alone (Figure 4C). However, furrow ingression in the doubly depleted embryos was slower than in Rho-kinase-depleted embryos (Figure 4G), and cytokinesis failed in 63% of cells (7/11 embryos; Figure 4F, diamonds mark the ends of traces for embryos that failed to complete cytokinesis). Thus, cytokinesis is insensitive to a decrease in contractility when septins are present and furrowing is asymmetric. But when ingression is symmetric due to septin inhibition and contractility is reduced by Rho-kinase depletion, cytokinesis fails at high frequency. The role of the septins in furrow asymmetry could be independent of their role in rendering cytokinesis insensitive to reduction of contractility. However, the extreme furrow asymmetry of Rho-kinase-depleted embryos, combined

(F) The kinetics of furrow closure were measured in embryos expressing GFP:MLC-4 as for Figure 1B. Averages are shown for controls and septin-depleted embryos; individual traces are shown for embryos simultaneously depleted of the septins and Rho-kinase and Rho-kinase alone. Diamonds mark the ends of traces and time of furrow regression for embryos that failed to complete cytokinesis.

(G) Rate of furrow closure between 80% and 20% starting width (gray box in [C]). Error bars = SEM; \* = < control,  $p < 0.005$ ;  $\phi$  = < Rho-kinase depleted,  $p < 0.02$ .

(H) Schematic summarizing the effect of depletion the septins, Rho-kinase, or both on myosin (red) abundance and distribution, and the rate and symmetry (gray arrows) of furrowing.

with the high failure rate when Rho-kinase-depleted embryos are forced to furrow symmetrically by septin depletion, lead us to favor the idea that furrow asymmetry renders the contractile ring robust to mechanical challenges.

In summary, our findings indicate that the contractile ring possesses an intrinsic symmetry-breaking mechanism to promote asymmetric furrowing. Central to this mechanism are two widely conserved contractile ring components, Anillin and the septins, that are molecularly well suited to coalesce the interacting network of filament systems in the contractile ring. Furrow asymmetry may serve a mechanical function, enhancing the robustness of cytokinesis. A second possible function for furrow asymmetry is suggested by the finding that in polarized epithelia, asymmetric furrowing occurs in a specific orientation relative to the axis of polarity (Reinsch and Karsenti, 1994) (Figure 1C), likely allowing maintenance of epithelial integrity during the division of its constituent cells. This result suggests that in some contexts, asymmetric ingression couples cell division to tissue architecture. The tissue morphogenesis defects that result from inhibition of the septins (Finger et al., 2003; Nguyen et al., 2000) and Anillin (Maddox et al., 2005) in *C. elegans* are consistent with such a function; however, direct monitoring of cytokinesis in intact tissues is needed to explore this possibility.

## EXPERIMENTAL PROCEDURES

### Strains

*C. elegans* strains (genotypes in Table S1) were maintained using standard procedures. The strain expressing NMY-2::GFP (Nance et al., 2003) was a gift of Edwin Munro. The strain expressing GFP::MoeABD, a GFP fusion with the F-actin binding domain of *Drosophila* moesin (PF100; Motegi et al., 2006), was provided by Nathalie Velarde and Fabio Piano.

### Microscopy

For all live imaging except for Figures S1 and S2, newly fertilized embryos were mounted as described (Oegema et al., 2001) and imaged at 20°C using a spinning disc confocal equipped with a 60 $\times$ , 1.40 NA Nikon PlanApo objective, and 2  $\times$  2 binning. For Figure S1, embryos were tipped into a depression in an agarose pad and oriented with their long axis parallel to the axis of the objective. For Figure S2, embryos were mounted without compression between two coverslips separated by a Vaseline spacer.

For end-on reconstructions, a 16-plane Z series at 2.5  $\mu$ m intervals was collected at each time point. Custom macros written for Metamorph software (Downingtown, PA) or DeltaVision (Applied Precision, Issaquah, WA) were used to rotate the data from the central region of the embryo containing the contractile ring by 90° and generate a maximum intensity projection. For single-plane confocal imaging, one image was acquired in the center Z plane of the embryo, where the spindle was maximally visible by DIC imaging as a clearing in the cytoplasm.

### RNA-Mediated Interference

Double-stranded RNAs (dsRNAs) were prepared as described (Oegema et al., 2001). DNA templates were prepared using primers (Table S2) to amplify regions of N2 genomic DNA or gene-specific cDNAs as indicated. L4-stage hermaphrodites were injected with dsRNA and incubated at 20°C for 45–48 hr for thorough depletions and 16–20 hr for partial depletions. For double depletions in Figures 2D and Figure S3, L4 hermaphrodites were first injected with the RNA targeting the gene whose product was to be fully depleted (Anillin

or septin). The injected worms were then incubated until 16–20 hr before imaging, when they were reinjected with an equal concentration mixture of the first dsRNA and dsRNA targeting *mlc-4*. For single depletions that served as controls for double depletions, target-gene dsRNAs were mixed with a control dsRNA directed against a *C. elegans* gene (*sas-5*) required only after the first division to control for mixing and dilution.

### Fluorescence Intensity Measurements

Measurements of the abundance of myosin (NMY-2::GFP) on the equatorial cortex during contractile ring assembly (Figures 2C and 2D; Figure S3) were made on maximum-intensity projections of four-plane Z series containing the embryo cortex. The total GFP intensity inside a box at the cell equator (solid-line box in Figure 2C) was measured, and the background in a same-sized region outside the contractile ring (dotted-line box in Figure 2C) was subtracted. Equatorial NMY-2::GFP intensity at anaphase onset was subtracted from all subsequent values to plot anaphase-specific myosin recruitment to the equatorial cortex.

For measurements of the asymmetry of GFP intensity around the contractile ring, only embryos in which ingression occurred along an axis parallel to the plane of the coverslip were analyzed. This allowed us to exclude artifacts due to sample depth, because the regions from the two sides of the embryos whose intensity was compared were at the same sample depth. Asymmetry measurements were made using end-on maximum intensity projections when the contractile ring was ~50% closed. Custom analysis journals created using Metamorph software (Universal Imaging Corp.) were used to measure the total fluorescence intensity in arcs spanning the top two quadrants of the contractile ring (Figure 3D). After subtracting the background in a same-sized region outside the contractile ring, the larger value was always divided by the smaller value.

### Supplemental Data

Three supplemental figures illustrate that asymmetric furrowing occurs in embryos not under compression, that the axis of furrowing in the first mitotic division does not correlate with the dorso-ventral axis, and that the septins are required for asymmetric furrowing over a wide range of myosin levels. Movie S1 accompanies Figure 2A and shows two views of asymmetric furrowing in a control embryo. Movie S2 shows that the axis of asymmetric furrowing is random with respect to the axis of compression. Movie S3 accompanies Figure S1. Movie S4 shows that furrowing is symmetric within the division plane following depletion of Anillin or the septins. The Supplemental Data are available at <http://www.developmentalcell.com/cgi/content/full/12/5/827/DC1/>.

### ACKNOWLEDGMENTS

We thank Yuji Kohara for gene-specific cDNAs, the *Caenorhabditis* Genome Center for strains and Nathalie Velarde and Fabio Piano for generously providing the *C. elegans* strain expressing GFP::moeABD ahead of publication. We are grateful to Paul Maddox for custom analysis journals and helpful discussion, Jon Audhya for *C. elegans* strains, and Julie Canman, Paul Maddox, Tae Hoon Kim, Lisa Cameron, Ana Carvalho, and Iain Cheeseman for thoughtful comments on the manuscript. A.S.M. is a fellow of the Giannini Family Foundation. L.L. is a graduate student in the Biomedical Sciences graduate program, supported by the University of California, San Diego, Genetics Training Grant. K.O. is a Pew Scholar in the Biomedical Sciences. A.D. is the Connie and Bob Lurie Scholar of the Damon Runyon Cancer Research Foundation. A.D. and K.O. also receive salary and additional support from the Ludwig Institute for Cancer Research.

Received: January 28, 2007  
Revised: February 22, 2007  
Accepted: February 26, 2007  
Published: May 7, 2007

## REFERENCES

- Adam, J.C., Pringle, J.R., and Peifer, M. (2000). Evidence for functional differentiation among *Drosophila* septins in cytokinesis and cellularization. *Mol. Biol. Cell* **11**, 3123–3135.
- Audhya, A., Hyndman, F., McLeod, I.X., Maddox, A.S., Yates, J.R., 3rd, Desai, A., and Oegema, K. (2005). A complex containing the Sm protein CAR-1 and the RNA helicase CGH-1 is required for embryonic cytokinesis in *Caenorhabditis elegans*. *J. Cell Biol.* **171**, 267–279.
- Berlin, A., Paoletti, A., and Chang, F. (2003). Mid2p stabilizes septin rings during cytokinesis in fission yeast. *J. Cell Biol.* **160**, 1083–1092.
- Echard, A., Hickson, G.R., Foley, E., and O'Farrell, P.H. (2004). Terminal cytokinesis events uncovered after an RNAi screen. *Curr. Biol.* **14**, 1685–1693.
- Field, C.M., and Alberts, B.M. (1995). Anillin, a contractile ring protein that cycles from the nucleus to the cell cortex. *J. Cell Biol.* **131**, 165–178.
- Field, C.M., al-Awar, O., Rosenblatt, J., Wong, M.L., Alberts, B., and Mitchison, T.J. (1996). A purified *Drosophila* septin complex forms filaments and exhibits GTPase activity. *J. Cell Biol.* **133**, 605–616.
- Field, C.M., Coughlin, M., Doberstein, S., Marty, T., and Sullivan, W. (2005). Characterization of anillin mutants reveals essential roles in septin localization and plasma membrane integrity. *Development* **132**, 2849–2860.
- Finger, F.P., Kopish, K.R., and White, J.G. (2003). A role for septins in cellular and axonal migration in *C. elegans*. *Dev. Biol.* **261**, 220–234.
- Frazier, J.A., Wong, M.L., Longtine, M.S., Pringle, J.R., Mann, M., Mitchison, T.J., and Field, C. (1998). Polymerization of purified yeast septins: evidence that organized filament arrays may not be required for septin function. *J. Cell Biol.* **143**, 737–749.
- Gladfelter, A.S., Pringle, J.R., and Lew, D.J. (2001). The septin cortex at the yeast mother-bud neck. *Curr. Opin. Microbiol.* **4**, 681–689.
- Glotzer, M. (2005). The molecular requirements for cytokinesis. *Science* **307**, 1735–1739.
- Gönczy, P., and Rose, L.S. (2006). Asymmetric cell division and axis formation in the embryo. In *Wormbook*, The *C. elegans* Research Community, ed. 10.1895/wormbook.1.30.1 (<http://www.wormbook.org>).
- Hartwell, L.H. (1971). Genetic control of the cell division cycle in yeast. IV. Genes controlling bud emergence and cytokinesis. *Exp. Cell Res.* **69**, 265–276.
- Kinoshita, M. (2006). Diversity of septin scaffolds. *Curr. Opin. Cell Biol.* **18**, 54–60.
- Kinoshita, M., Field, C.M., Coughlin, M.L., Straight, A.F., and Mitchison, T.J. (2002). Self- and actin-templated assembly of Mammalian septins. *Dev. Cell* **3**, 791–802.
- Longtine, M.S., DeMarini, D.J., Valencik, M.L., Al-Awar, O.S., Fares, H., De Virgilio, C., and Pringle, J.R. (1996). The septins: roles in cytokinesis and other processes. *Curr. Opin. Cell Biol.* **8**, 106–119.
- Maddox, A.S., Habermann, B., Desai, A., and Oegema, K. (2005). Distinct roles for two *C. elegans* anillins in the gonad and early embryo. *Development* **132**, 2837–2848.
- Matsumura, F. (2005). Regulation of myosin II during cytokinesis in higher eukaryotes. *Trends Cell Biol.* **15**, 371–377.
- Motegi, F., Mishra, M., Balasubramanian, M.K., and Mabuchi, I. (2004). Myosin-II reorganization during mitosis is controlled temporally by its dephosphorylation and spatially by Mid1 in fission yeast. *J. Cell Biol.* **165**, 685–695.
- Motegi, F., Velarde, N.V., Piano, F., and Sugimoto, A. (2006). Two phases of astral microtubule activity during cytokinesis in *C. elegans* embryos. *Dev. Cell* **10**, 509–520.
- Nance, J., Munro, E.M., and Priess, J.R. (2003). *C. elegans* PAR-3 and PAR-6 are required for apicobasal asymmetries associated with cell adhesion and gastrulation. *Development* **130**, 5339–5350.
- Neufeld, T.P., and Rubin, G.M. (1994). The *Drosophila* peanut gene is required for cytokinesis and encodes a protein similar to yeast putative bud neck filament proteins. *Cell* **77**, 371–379.
- Nguyen, T.Q., Sawa, H., Okano, H., and White, J.G. (2000). The *C. elegans* septin genes, *unc-59* and *unc-61*, are required for normal post-embryonic cytokinesis and morphogenesis but have no essential function in embryogenesis. *J. Cell Sci.* **113**, 3825–3837.
- Oegema, K., Savoian, M.S., Mitchison, T.J., and Field, C.M. (2000). Functional analysis of a human homologue of the *Drosophila* actin binding protein anillin suggests a role in cytokinesis. *J. Cell Biol.* **150**, 539–552.
- Oegema, K., Desai, A., Rybina, S., Kirkham, M., and Hyman, A.A. (2001). Functional analysis of kinetochore assembly in *Caenorhabditis elegans*. *J. Cell Biol.* **153**, 1209–1226.
- Piekny, A.J., and Mains, P.E. (2002). Rho-binding kinase (LET-502) and myosin phosphatase (MEL-11) regulate cytokinesis in the early *Caenorhabditis elegans* embryo. *J. Cell Sci.* **115**, 2271–2282.
- Rappaport, R. (1996). *Cytokinesis in Animal Cells*, 1st Edition (Cambridge, UK: Cambridge University Press).
- Reinsch, S., and Karsenti, E. (1994). Orientation of spindle axis and distribution of plasma membrane proteins during cell division in polarized MDCKII cells. *J. Cell Biol.* **126**, 1509–1526.
- Robinson, D.N., and Spudich, J.A. (2004). Mechanics and regulation of cytokinesis. *Curr. Opin. Cell Biol.* **16**, 182–188.
- Rodal, A.A., Kozubowski, L., Goode, B.L., Drubin, D.G., and Hartwig, J.H. (2005). Actin and septin ultrastructures at the budding yeast cell cortex. *Mol. Biol. Cell* **16**, 372–384.
- Satterwhite, L.L., and Pollard, T.D. (1992). Cytokinesis. *Curr. Opin. Cell Biol.* **4**, 43–52.
- Sohrmann, M., Fankhauser, C., Brodbeck, C., and Simanis, V. (1996). The *dmf1/mid1* gene is essential for correct positioning of the division septum in fission yeast. *Genes Dev.* **10**, 2707–2719.
- Somma, M.P., Fasulo, B., Cenci, G., Cundari, E., and Gatti, M. (2002). Molecular dissection of cytokinesis by RNA interference in *Drosophila* cultured cells. *Mol. Biol. Cell* **13**, 2448–2460.
- Straight, A.F., Field, C.M., and Mitchison, T.J. (2005). Anillin binds non-muscle myosin II and regulates the contractile ring. *Mol. Biol. Cell* **16**, 193–201.
- Tasto, J.J., Morrell, J.L., and Gould, K.L. (2003). An anillin homologue, Mid2p, acts during fission yeast cytokinesis to organize the septin ring and promote cell separation. *J. Cell Biol.* **160**, 1093–1103.
- Versele, M., and Thorner, J. (2005). Some assembly required: yeast septins provide the instruction manual. *Trends Cell Biol.* **15**, 414–424.
- Vrabiou, A.M., and Mitchison, T.J. (2006). Structural insights into yeast septin organization from polarized fluorescence microscopy. *Nature* **443**, 466–469.
- Zhao, W.M., and Fang, G. (2005). Anillin is a substrate of anaphase-promoting complex/cyclosome (APC/C) that controls spatial contractility of myosin during late cytokinesis. *J. Biol. Chem.* **280**, 33516–33524.